THE 1994–1995 MANYARA AND KWAMTORO EARTHQUAKE SWARMS: VARIATION IN THE DEPTH EXTENT OF SEISMICITY IN NORTHERN TANZANIA

G.D. MULIBO
Department of Geosciences, The Pennsylvania State University, University Park, Pennsylvania 16802, USA
email: gmulibo@geosc.psu.edu

A.A. NYBLADE
Department of Geosciences, The Pennsylvania State University, University Park, Pennsylvania 16802, USA
University of the Witwatersrand, Private Bag 3, WITS, 2050 South Africa
email: andy@geosc.psu.edu

© 2009 December Geological Society of South Africa

ABSTRACT

Seismicity within two earthquake swarms (m_b 1.0 to 4.0) in northern Tanzania recorded by the 1994-1995 Tanzania Broadband Seismic Experiment has been investigated through event relocation, modelling of regional depth phases and examination of focal mechanisms. In the Manyara swarm, seismicity is distributed over a region ~20 km wide and extends to >30 km depth. Hypocenters correlate well with the Manyara Rift, and focal mechanisms of many events show normal faulting with nodal planes having the same north-northeast orientation as the Manyara Rift border fault. This result indicates that the events are consistent with slip along the border fault and related faults beneath the Manyara Rift, and shows that the faults extend into the lower crust. Seismicity in the KwaMtoro swarm is distributed over a region ~10 km wide but extends only to ~12 km depth. There are no mapped faults above the swarm, but a strong correlation between the north to south orientation of the swarm, the north to south orientation of nodal planes in focal mechanisms, and north to south striking extensional structures nearby, suggest that events in this swarm could be caused by slip on a system of rift faults. However, a magma-driven origin for either swarm cannot be ruled out either.

Introduction

In northern Tanzania, the Eastern Branch of the East African Rift System (EARS) impinges on the eastern margin of the Archean Tanzania Craton in a region of incipient rifting (e.g., Wohlenberg, 1969; Fairhead and Stuart, 1982; Dawson, 1992) (Figure 1). Previous seismicity studies identified two earthquake swarms, with m_b 1.0 to 4.0, that were active within northern Tanzania in 1994 and 1995, one in the Manyara Rift, referred to as the Manyara swarm, and the other one to the south of the Manyara Rift along the edge of the craton, referred to as the KwaMtoro swarm (Nyblade et al., 1996; Langston et al., 1998). Preliminary hypocentral locations indicated that most of the seismicity in these swarms occurred within the upper and middle part of the crust, but that some events could be as deep as 40 km. However, the preliminary hypocenters were not well constrained, leaving much uncertainty about the depth extent and location of the seismicity in relationship to nearby rift structures. Through event relocation, modelling of regional depth phases and examination of focal mechanisms, we investigate if these swarms are consistent with slip on rift faults, if seismicity does indeed extend into the lower crust, and if these swarms could also be attributed to dike-induced faulting.

Geology and tectonic setting

The East African Plateau, covering an area of ~1.8 x 10^6 km^2 with a mean elevation of about 1 km, has been described as a first order topographic feature within the African continent (Nyblade and Robinson, 1994; Burke, 1996). The plateau encompasses several Precambrian terrains that have experienced Cenozoic extension related to uplift and rifting across East Africa (Figure 1). These terrains include the Archean Tanzania Craton, located in the centre of the plateau, surrounded by the Proterozoic Mozambique, Ubendian and Kibaran Belts. The ~3000 km long Cenozoic Rift System forms two branches, namely, the Western Branch and the Eastern Branch that have developed within the mobile belts along the flanks of the plateau (Figure 1).

The rift structures within northern Tanzania define the termination of the Eastern Branch (Figure 2), and this termination is marked by a change in the rift morphology. As it enters northern Tanzania, the Eastern Branch splays into a ~300 km wide zone of block faulting, in contrast to the well-defined, 80 km wide graben it forms to the north in Kenya. The 300 km wide zone can be divided into three distinct segments defined by the Eyasi rift to the west, the Manyara Rift in the middle and the Pangani rift to the east (Figure 2). The three segments consist of many half graben structures up to 100 km long and 50 km wide, often bordered by a pronounced escarpment (Foster et al., 1997). The zone of block faulting is also characterised by several volcanoes (Figure 2). The divergence of the rift may be caused by the presence of thick cratonic lithosphere extending beneath the Mozambique Belt in northern Tanzania (Ebinger et al., 1997; Nyblade and Brazier, 2002).

The middle rift segment in northern Tanzania extends ~400 km south and south-westward along the edge of the craton (Tesha et al., 1997; Figure 2). The earthquake swarms investigated in this study lie within this middle segment (Figure 2). The northern, or

doi:10.2113/gssajg.112.3-4.387

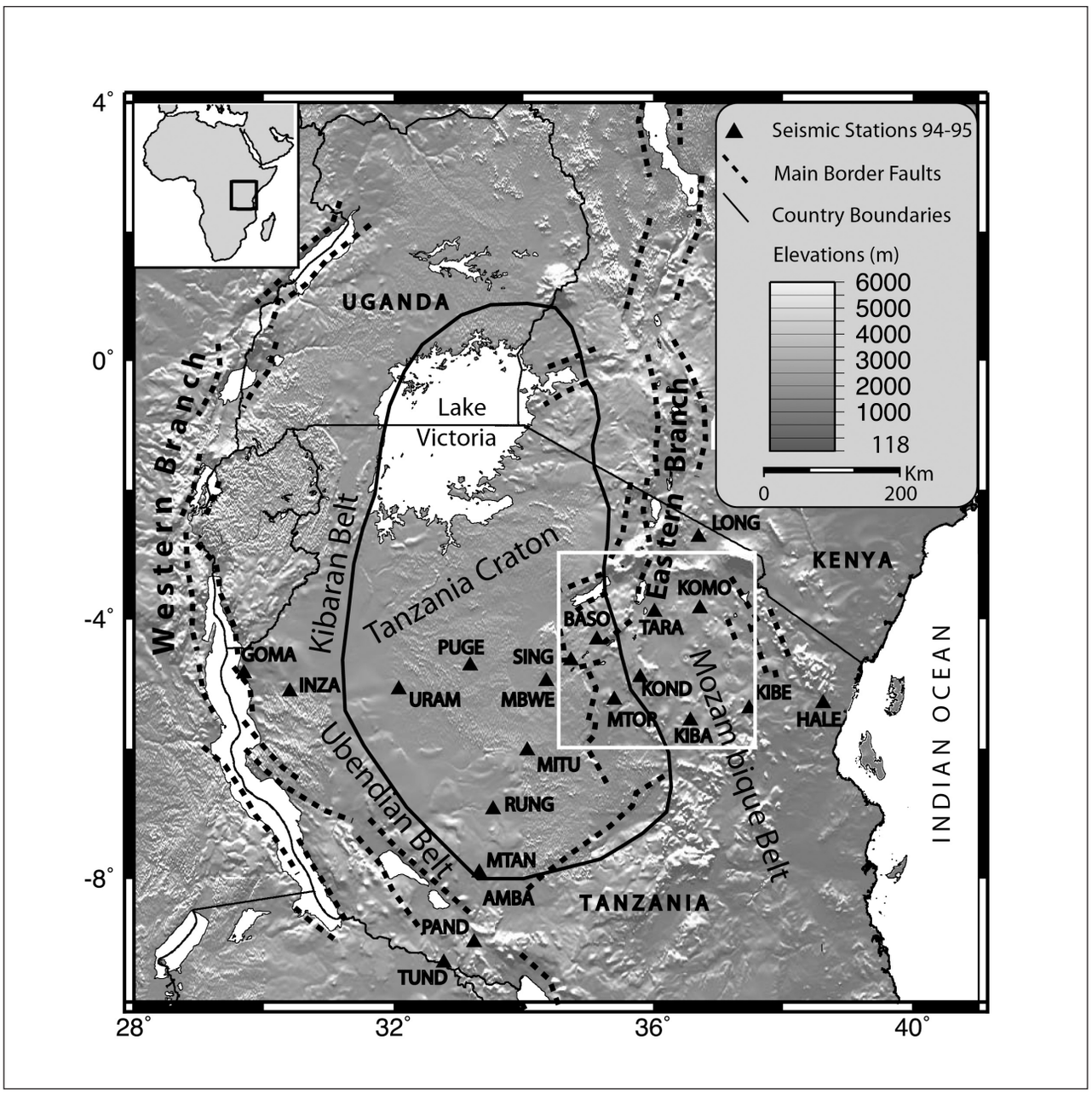


Figure 1. *Map showing regional geology of east Africa, including the Tanzania Craton (solid bold line), the Proterozoic mobile belts surrounding the craton, and the major Cenozoic rift faults (bold dashed lines) of the East African Rift system. The locations of seismic stations used in the study are shown as triangles. The white rectangle marks the location of Figure 2.*

Manyara swarm, developed adjacent to the ~100 km long Manyara Rift border fault. This border fault displays a segmented geometry characteristic of many continental rift faults (Ebinger et al., 1993), has an average dip of 60° (Ring et al., 2005; Le Gall et al., 2008) and forms a ~500 m high escarpment.

The southern, or KwaMtoro swarm, lies almost directly south of the Manyara swarm in an area where there are no mapped faults. The geological map and the Shuttle Radar Topography Mission (SRTM) data of the area show nearby morphological features associated with faults and topographic lineaments trending in sub northsouth to north-northeast to south-southwest directions (Figures 2 and 3). Some of these faults are likely to be Plio-Pleistocene in age (Fozzard, 1961). The area is bordered to the west and southwest by the Chenene Mountains (~2.0 km high), to the northwest by the Plio-Pleistocene Hanang volcanic complex (~3.4 km high), and to the east by the Masai Block (Figures 2 and 3). The Chenene Mountains are also referred to as the KwaMtoro block.

Previous studies of seismicity and focal mechanisms

Seismicity maps of East Africa produced over the past few decades show that most of the seismicity is confined



Figure 2. *Sketch map showing the geology and tectonics of the study area and the location of the two earthquake swarms investigated in this study (**A** and **B**), and the Gelai swarm (**C**) (Calais et al., 2009). The map also shows the three rift segments of the northern Tanzania divergence zone along with the volcanic centers (modified from Ring et al., 2005 and Macheyeki et al., 2008).*

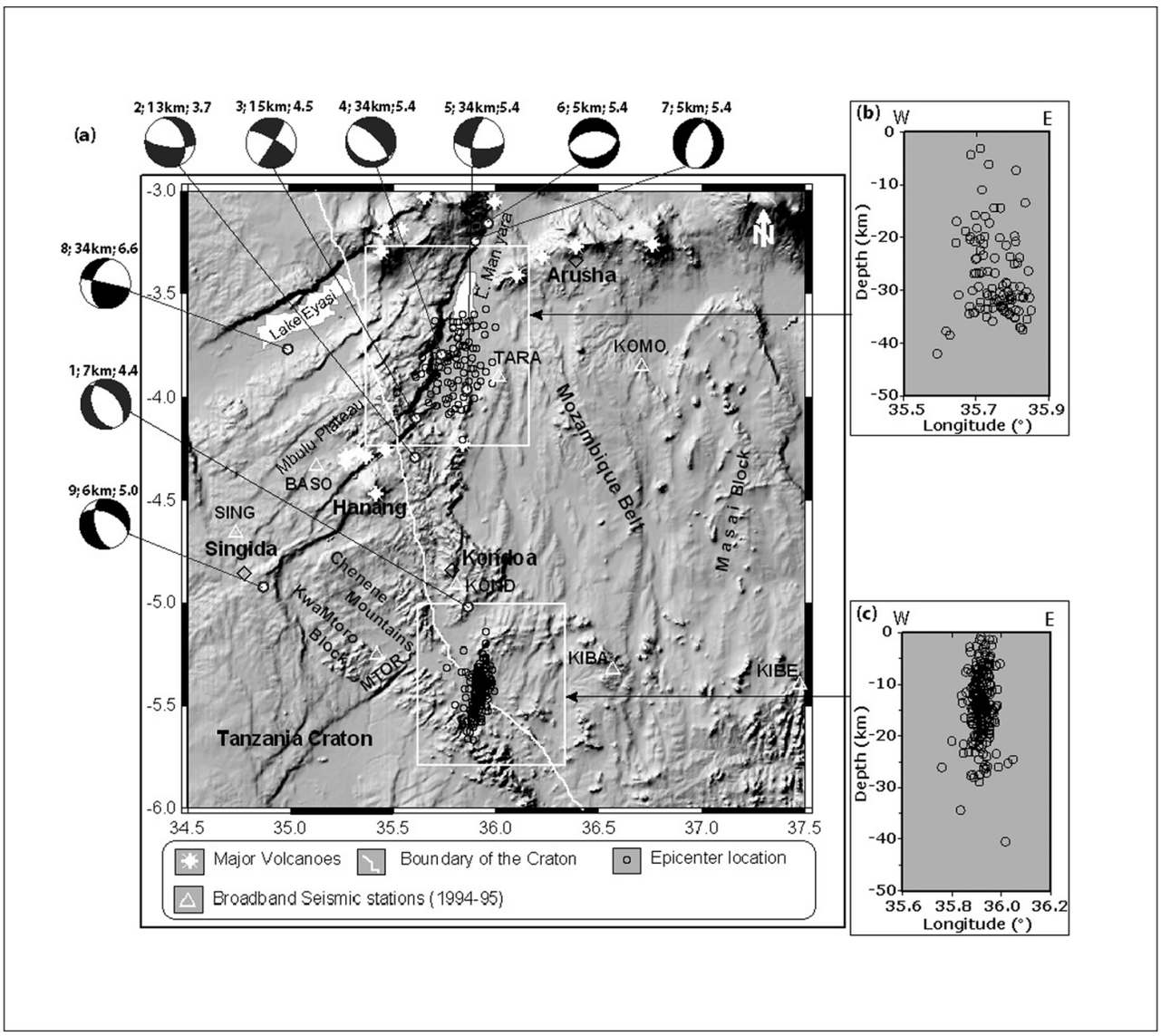


Figure 3 *(**a**). The Satellite Radar Topography Mission (SRTM) map with 90 m resolution (Sun elevation 45°) showing the location of the Manyara and KwaMtoro earthquake swarms recorded during the one-year Tanzania broadband seismic experiment (1994-95). The white rectangles mark the locations of Figures 6 and 7. Epicenters shown are from Nyblade et al. (1996) and Langston et al. (1998). Numbers on focal mechanisms show event number, source depth and magnitude. Events 1 to 5 are from Brazier et al. (2005); 6 and 7, Foster and Jackson (1998); 8, Nyblade and Langston (1995); 9, Shudofsky (1985). (**b**) West to east cross-section of the Manyara swarm. (**c**) West to east cross-section of the KwaMtoro swarm. The thin white line shows the exposed eastern margin of the Tanzania Craton.*

to the rift zones (Figure 4), (e.g., Fairhead and Girdler, 1969; Wohlenberg, 1969; Bungum and Nnko, 1984; Kebede and Kulhanek, 1991; Iranga, 1992; Nyblade et al., 1996). The highest amount of seismicity in the Eastern branch occurs in northern Tanzania, encompassing the area of the earthquake swarms investigated here.

Studies of the depth distribution of seismicity within the East African Rift, including northern Tanzania, have reported events throughout the upper and lower crust (e.g., Shudofsky et al., 1987; Nyblade and Langston, 1995; Foster and Jackson, 1998; Langston et al., 1998). Well-constrained focal depths from waveform analysis using teleseismic data for events in northern Tanzania show nucleation depths extending to 30 to 40 km (Nyblade and Langston, 1995; Foster and Jackson, 1998). A study by Brazier et al. (2005) using regional depth phases obtained a focal depth of 34 km for an event within the Manyara rift (Figure 3).

Recent studies of an earthquake swarm (M>4) in the Gelai region of northern Tanzania (Figure 2) using seismic and geodetic data have suggested that the seismicity is associated with dyke-induced faulting (Baer et al., 2008; Calais et al., 2009). Events within the swarm extend to a depth of 14 km depth (Calais et al., 2009).

Focal mechanisms have been used in many studies to investigate the state of stress in the EARS. Results for the Eastern Branch suggest extension directions either

east-west, roughly perpendicular to the EARS trend (Fairhead and Stuart, 1982) or northwest-southeast, somewhat oblique to the EARS trend (Strecker et al., 1990). In northern Tanzania, focal mechanisms show a range of stress orientations (Shudofsky, 1985; Brazier et al., 2005). A recent study by Macheyeki et al. (2008) using a stress tensor inversion of focal mechanisms for events with m_b >4.0 in the Manyara rift found a nearly east-west extensional regime.

Data and methodology

Data

The data used in this study are from the one-year-long (1994–1995) Tanzania broadband seismic experiment that consisted of 20 broadband seismographs deployed in two 1000 km long linear arrays, one crossing Tanzania from the northeast to the southwest and the other crossing Tanzania from east to west (Nyblade et al., 1996; Figure 1). The distance between the stations ranged from 50 km to 200 km. Further details of the deployment can be found in Nyblade (1996).

Earthquake location

Events associated with the Manyara and KwaMtoro earthquake swarms were initially identified in the seismicity studies by Nyblade et al. (1996) and Langston et al. (1998). As noted previously, the event locations in these studies, and in particular focal depths, were not well constrained. To better resolve the seismicity patterns in the swarms, the events were relocated using both absolute and relative earthquake location techniques. A velocity model from Langston et al. (2002) (Table 1) was used in the location procedure for all stations. This model was chosen because it is the best

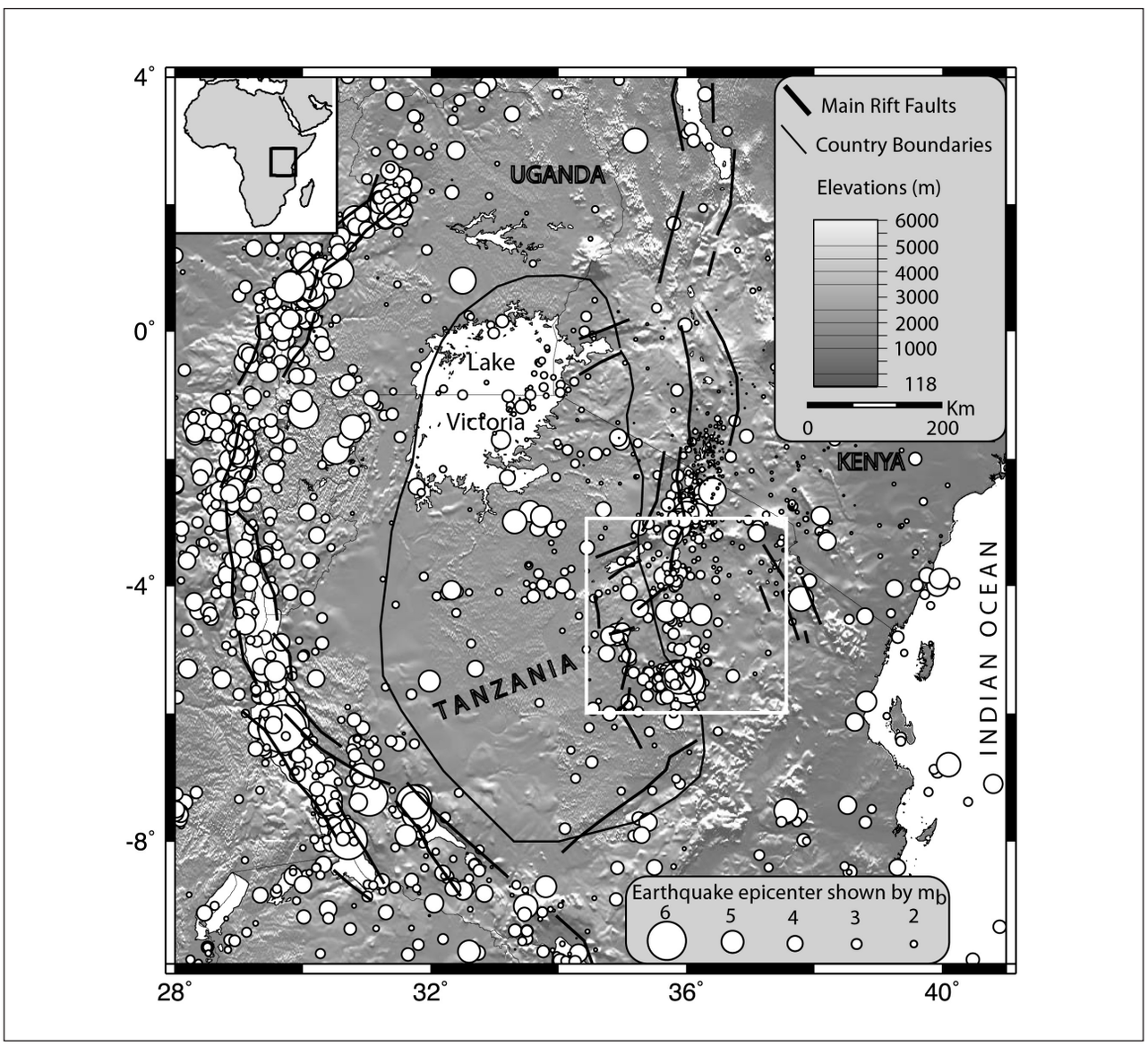


Figure 4. *Map showing seismicity (magnitude 2 to 6.5) for the East African rift system compiled from the International Seismological Center (ISC) catalogue for the period 1960–2008. The geology is the same as in Figure 1. The insert box is enlarged in Figure 3.*

Table 1. Velocity model from Langston et al. (2002) used for event location and for regional waveform modeling.

Layer thickness (km)	P-wave Vel. (km/s)	S-wave Vel. (km/s)	Density (g.cm^{-3})
10	5.84	3.38	2.33
10	6.26	3.62	2.50
10	6.68	3.86	2.67
7	7.09	4.10	2.84
Half space	8.28	4.74	3.31

available average crustal model for Precambrian terrains in Tanzania.

Absolute locations were obtained using handpicked P arrival times and the HYPOELLIPSE event location code (Lahr, 1999). The location procedure in HYPOELLIPSE is based on the minimisation of the root mean square (RMS) residuals obtained from phase arrival times (Lahr, 1999). Data from at least ten stations were used for locating each event. Uncertainty in the locations obtained arises primarily from picking arrival times, the velocity model and network geometry. Some of the P-wave arrivals in the data were very clear before filtering and others were not. Because of this, we filtered all the data using a band-pass filter of 1 to 5 Hz (Figure 5). On the filtered traces, P arrival times were picked to within 0.1s. S-phases were not easily picked on most of the records and thus S arrival times were not used in locating the events.

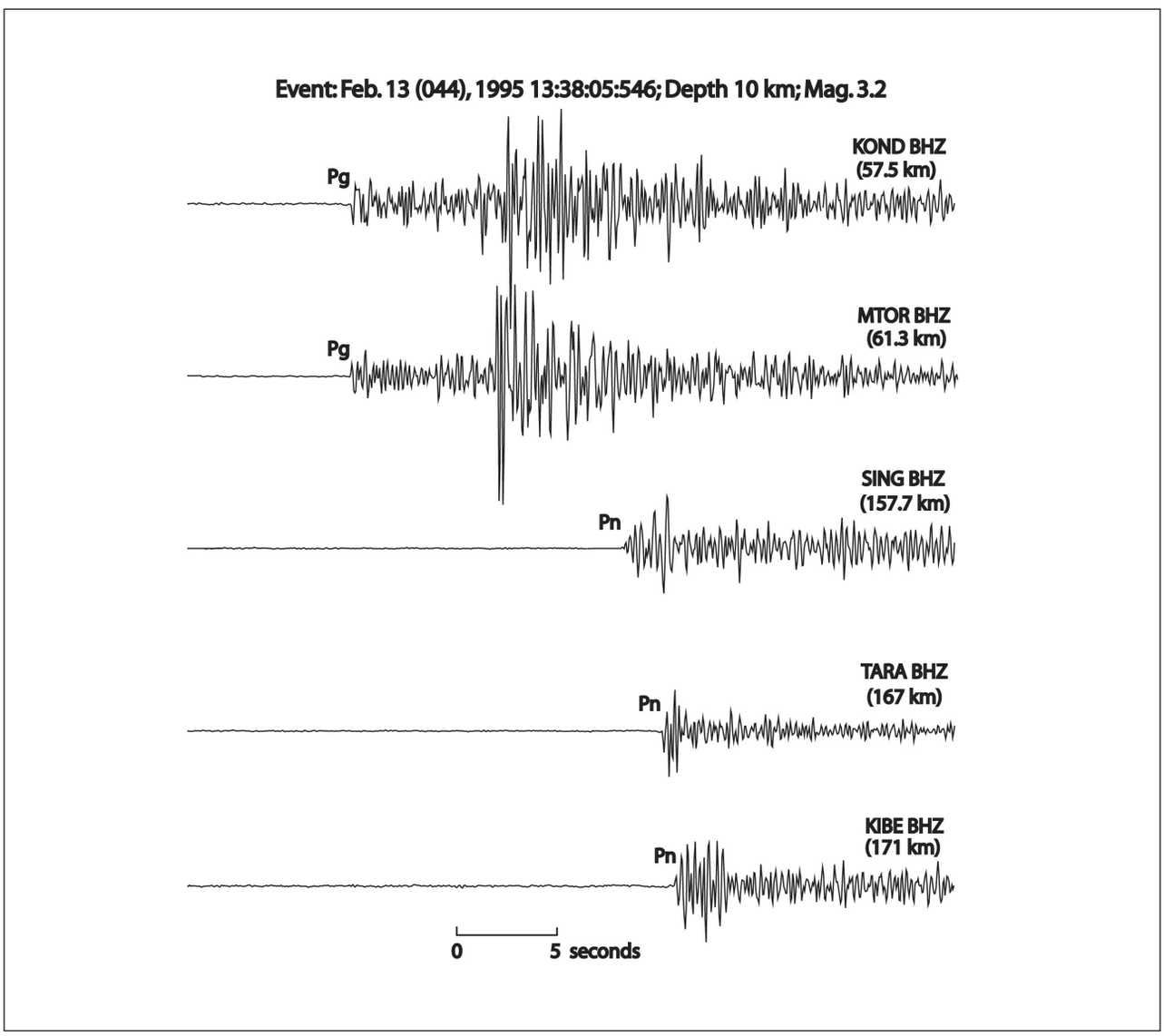


Figure 5. *Examples of band-pass (1-5 Hz) filtered vertical component velocity seismograms showing the onset of the first P-wave arrival for one event. All traces are aligned with the event origin time. The numbers above the seismograms give epicentral distances.*

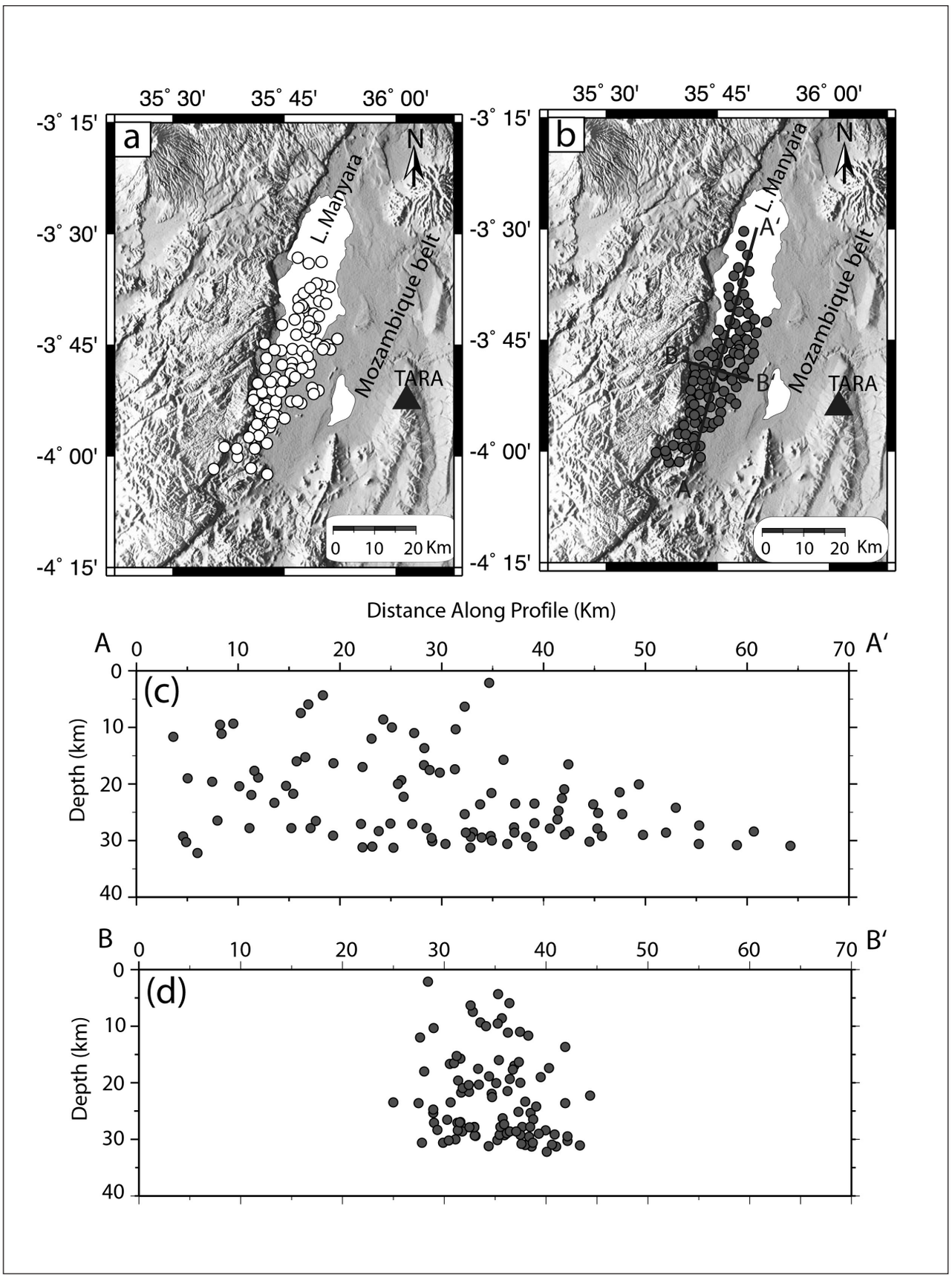


Figure 6. *Seismicity of the Manyara swarm. (**a**) Spatial distribution of earthquakes located using HYPOELLIPSE. (**b**) Spatial distribution of earthquakes located using hypoDD. (**c**) Cross-section A-A' showing depth distribution of the events drawn parallel to the cluster as shown in (b). (**d**) Cross-section B-B' showing depth distribution of the events drawn perpendicular to the cluster as shown in (b).*

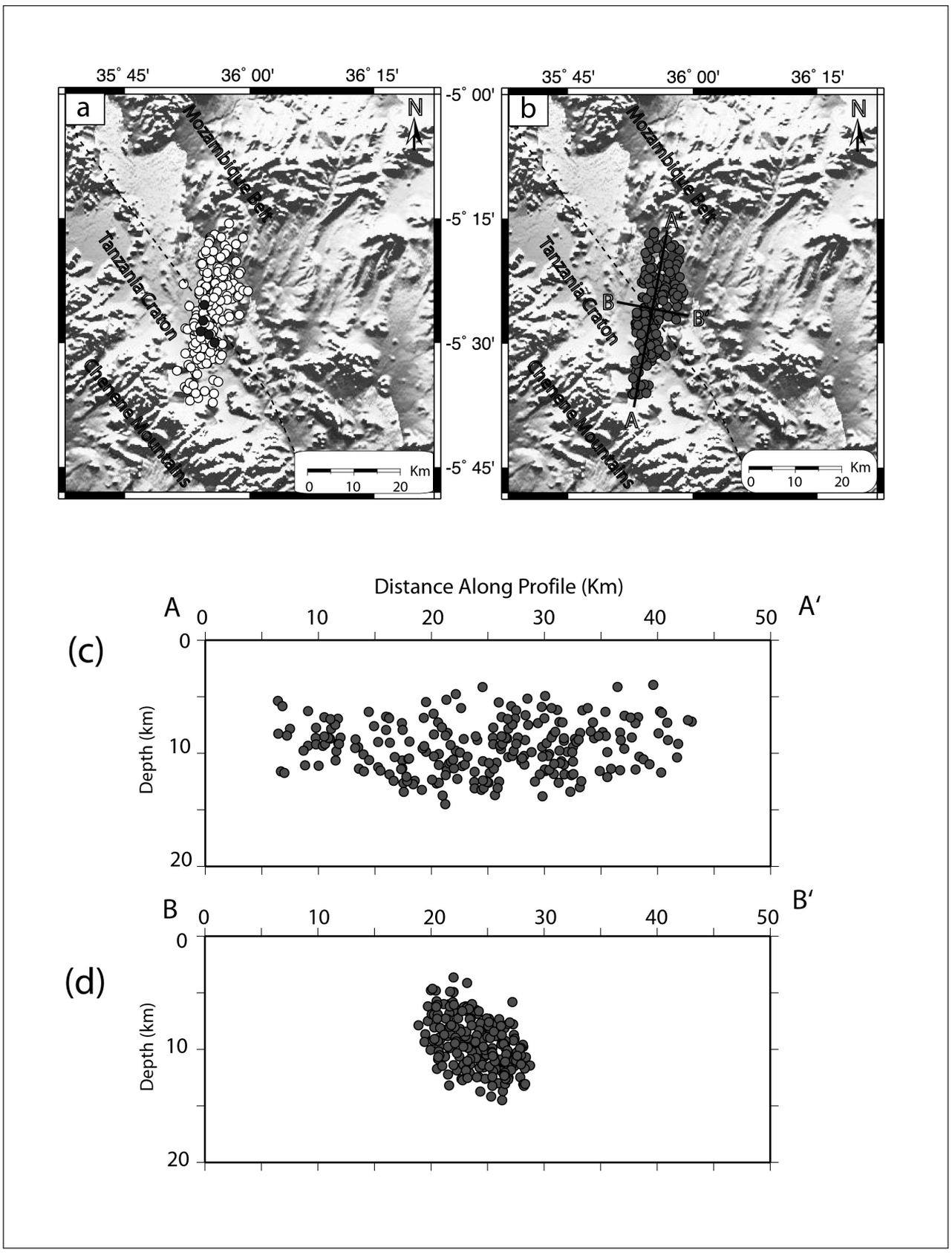


Figure 7. *Seismicity of the KwaMtoro swarm. (**a**) Spatial distribution of earthquakes located using HYPOELLIPSE. Black circles indicate the location of similar waveforms presented in Figure 10. (**b**) Spatial distribution of earthquakes located using hypoDD. (**c**) Cross-section A-A' showing depth distribution of the events drawn parallel to the cluster as shown in (b). (**d**) Cross-section B-B' showing depth distribution of the events drawn perpendicular to the cluster as shown in (b).*

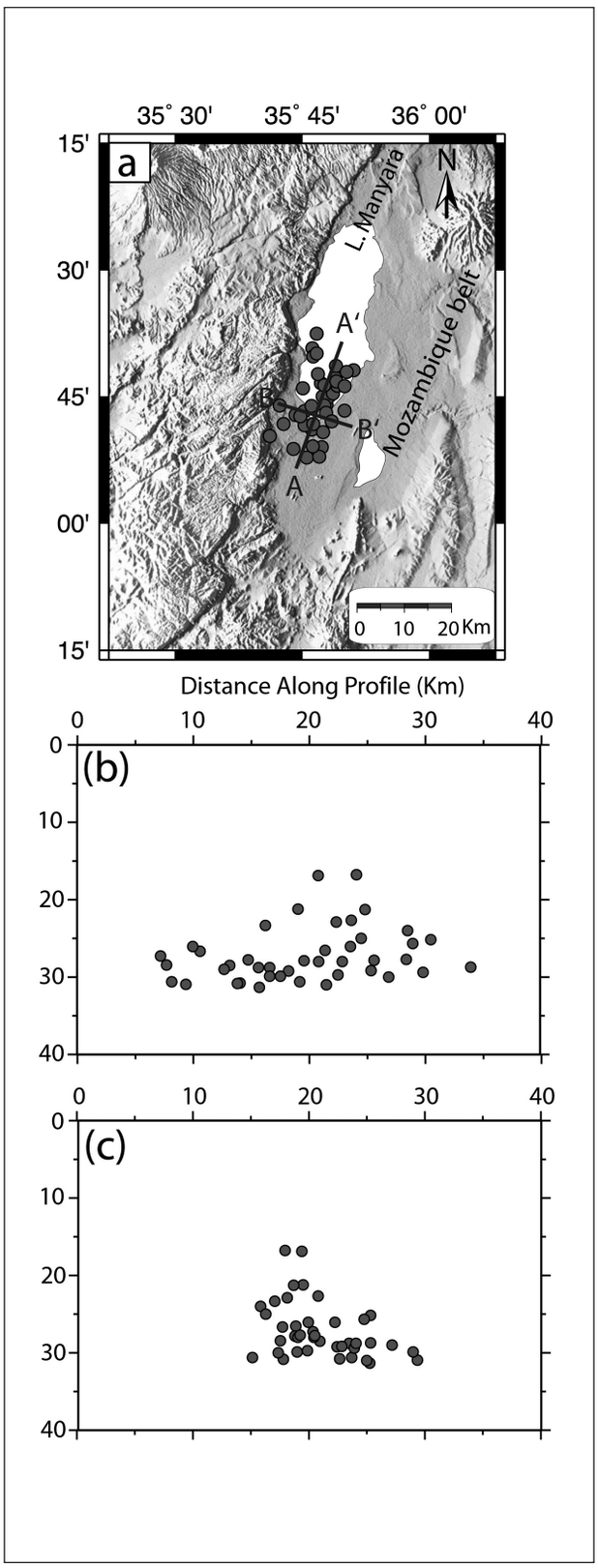


Figure 8. *Seismicity of the Manyara swarm. (**a**) Spatial distribution of earthquakes located using hypoDD with a correlation length of 5 km. (**b**) Cross-section A-A' showing depth distribution of the events drawn parallel to the cluster as shown in (a). (**c**) Cross-section B-B' showing depth distribution of the events drawn perpendicular to the cluster as shown in (a).*

In the location process, the P-wave picks that resulted in residuals between 0.8 s to 1.0 s were down weighted by 50 to 75% in the location algorithm, while those with residuals greater than 1.0 s were removed from the data set. Events with an average P travel time residual of less than 0.4 s were kept for further analysis and interpretation. The 68% confidence error ellipses obtained from the location procedure indicate that uncertainties in epicentral locations range from 0.5 to 1.6 km, and that uncertainties in the source depth range from 0.8 to 1.8 km. An event catalog is provided in Mulibo (2009).

To characterise further the pattern of seismicity in each swarm, we relocated the events using the relative location double-differencing code, hypoDD (Waldhauser and Ellsworth, 2000). The hypoDD technique uses arrival time differences to compute the relative position of neighboring events. It provides reliable relative hypocenter locations by exploiting the fact that the distance between events should be smaller than the distance between the events and stations. The method assumes that the ray path from an event to a station is independent of the un-modeled velocity perturbations along the ray path. The method further links events sharing one station by reducing the difference in travel time residual between pairs of events.

Event pairs were linked using a range of correlation lengths from 2 to 15 km recorded by stations within 300 km of the centre of the cluster. With smaller values (2 to 7 km), the double difference algorithm rejected larger numbers of events (60% to 90%), while for larger values (10 to 15 km), no differences in locations were obtained compared to the locations obtained from the HYPOELLIPSE code. The uncertainties in relative locations after using the double difference method, independent of correlation length, are 0.1 to 0.5 km horizontally and 0.1 to 0.4 km vertically.

Focal mechanisms

Fault plane solutions were obtained using the FOCMEC program (Snoke, 2003). The programme is based on a grid search through all combinations of strike, dip and rake to find the triplet of angles that best matches a given set of phase polarities. P-polarities only were used, along with a 2° angle increment in the grid search. Events for which one consistent set of nodal planes with an average uncertainty in strike, dip and rake of ≤5° were kept for interpretation. Using the full set of acceptable solutions for each event, an average mechanism was obtained. The full range of solutions for each event is given in Mulibo (2009).

Waveform modeling

To evaluate the source depths obtained from the relocation procedures, regional depth phases were modeled for a few of the deepest events in each swarm with synthetic seismograms computed using the reflection-matrix method (Kennett, 1983). In this method, the focal mechanism obtained for each event

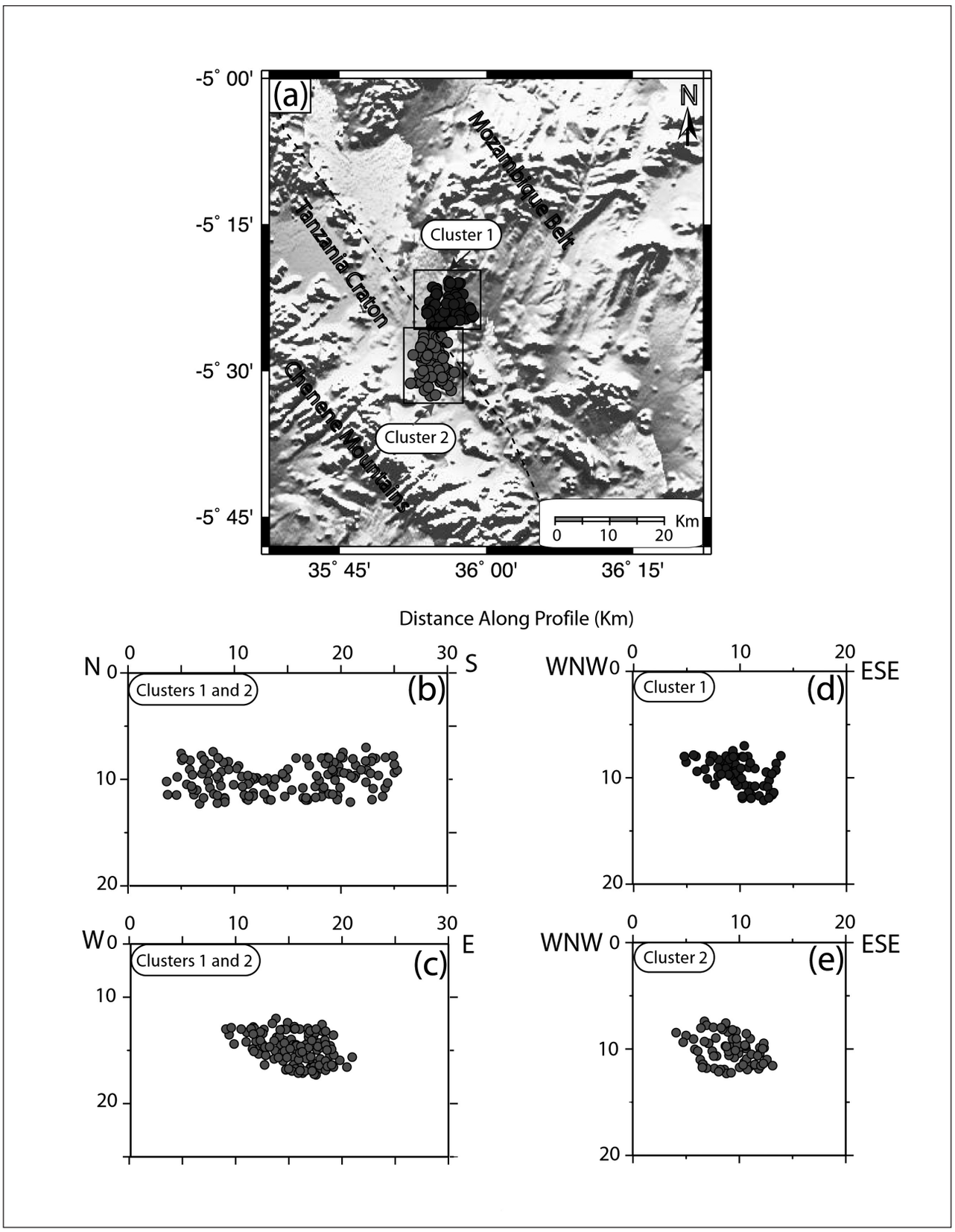


Figure 9. *Seismicity of the KwaMtoro swarm. (**a**) Spatial distribution of earthquakes located using hypoDD with a correlation length of 2 km. (**b**) North to south cross-section showing depth distribution of the events in clusters 1 and 2. (**c**) West to east cross-section showing depth distribution of the events in clusters 1 and 2. (**d**) Cross-section showing depth distribution of the events drawn perpendicular (west-northwest to east-southeast) to the cluster 1. (**e**) Cross-section showing depth distribution of the events drawn perpendicular (west-northwest to east-southeast) to the cluster 2.*

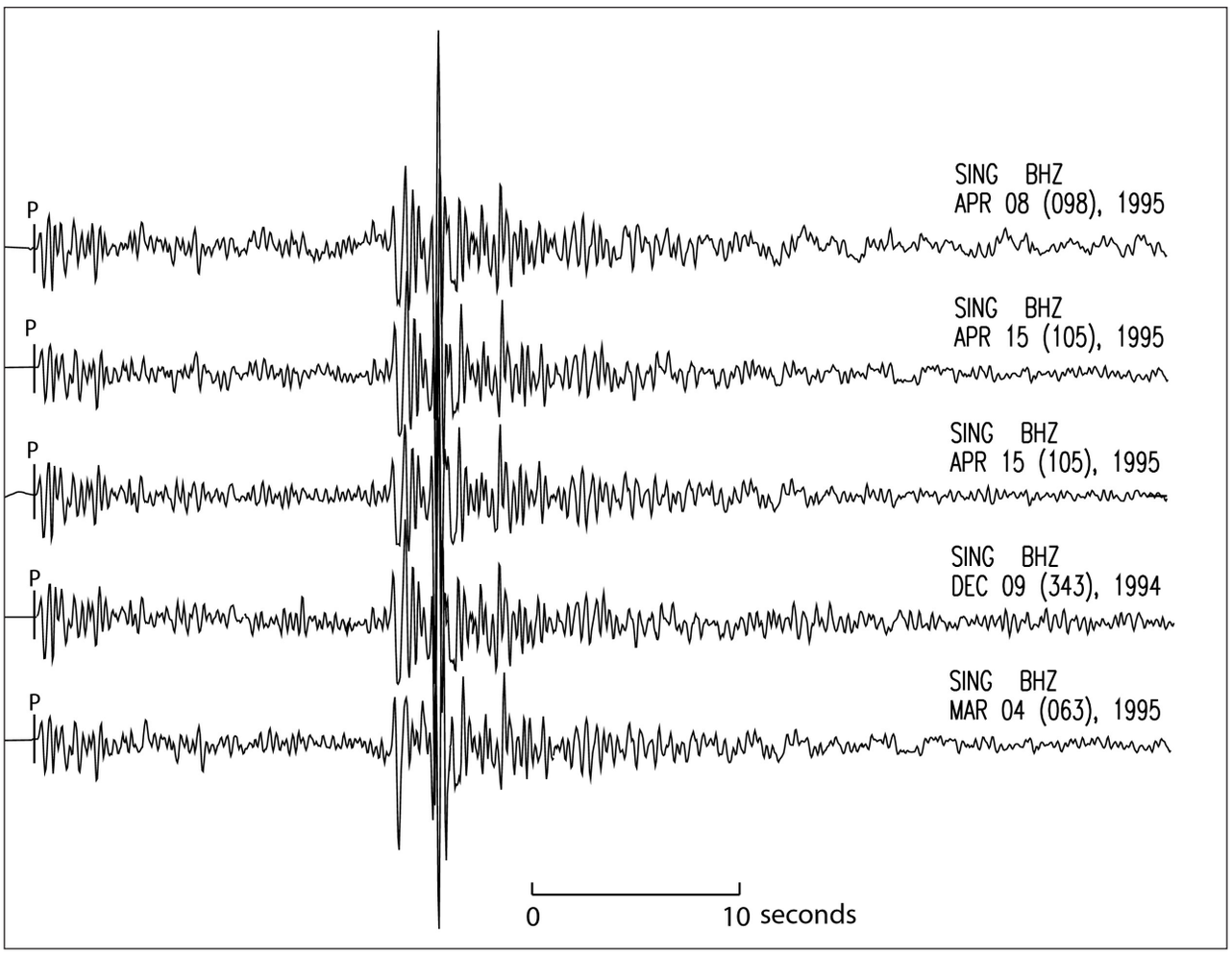


Figure 10. *Vertical velocity seismograms for selected events at station SING from the KwaMtoro swarm showing similar waveforms. The traces are aligned with the first P arrival and band pass filtered from 0.5 to 5 Hz.*

was used, together with the velocity model from Langston et al. (2002), to generate synthetic waveforms.

Synthetic seismograms generated for a range of source depths were then visually compared to the data for identifying and matching up regional depth phases (e.g., pPn, sPn, sSn), thereby constraining the focal depth. Arrival times for the depth phases were computed using the velocity model in Table 1 and the Tau-P code (Crotwell et al., 1999). We focused primarily on identifying and modeling sPn because Langston et al. (2002) show that this depth phase is a prominent phase on regional seismograms recorded at a distance ≥180 km within the study area. By matching the depth phases, source depths can be determined to ± 1 km.

Results

Event location using HYPOELLIPSE

A total of 313 events in both swarms were located using HYPOELLIPSE, 102 events in the Manyara swarm and 211 in the KwaMtoro swarm. The spatial pattern of the events in the Manyara swarm shows that the events are distributed within the Manyara Rift basin in a ~60 km long north-northeast to south-southwest striking swath (Figure 6a). The temporal distribution of the events does not show any correlation along the basin. The pattern of seismicity during any two-month interval is distributed along the entire length of the swath. The KwaMtoro swarm is shown in Figure 7a. Events in this cluster are spatially distributed in an almost north to south direction over a distance of ~45 km. As in the Manyara swarm, there is no temporal pattern in the distribution of the events along strike.

Event location using hypoDD

The spatial distribution of the epicenters obtained for the Manyara swarm from the hypoDD code, using a correlation length of 8 km, is somewhat more tightly clustered compared to the distribution obtained using the HYPOELLIPSE method (Figure 6a; b). From Figure 6, it can be seen that the events closely align with the Manyara Rift border fault. Cross-sections of the events running parallel and perpendicular to the cluster are illustrated in Figures 6c and d. From these cross-sections, it is clear that the earthquakes are distributed throughout the crust down to 30 to 33 km depth, with most of the events occurring between 15 to 30 km depth.

The epicenters obtained from the hypoDD code for the KwaMtoro swarm using a correlation length of 8 km (Figure 7b) also only show a small improvement in the clustering of hypocenters compared to the HYPOELLIPSE locations (Figures 7a and b). The spatial pattern of earthquakes in the KwaMtoro swarm cannot be correlated directly with mapped surface faults but clearly aligns with rift-related structures in the Masai Block (Figures 3 and 7b). The depth distribution of the earthquakes in this swarm is shallower than in the Manyara swarm (Figures 7c and d). Most of the events are concentrated in the crust between 8 to 12 km depth.

Different correlation lengths were used in the hypoDD code in an attempt to tighten up the clustering of hypocenters. For the Manyara swarm, a 5 km correlation length was found to be the smallest useful length. 90% of the events were rejected when smaller lengths were used (Figure 8). For the KwaMtoro swarm, a 2 km correlation length was found to be the smallest useful length (Figure 9). Reducing the correlation length for both swarms does not significantly improve the alignment of the hypocenters, and by adjusting the correlation lengths, we were unable to get the seismicity of either swarm align along a plane. Thus, the seismicity pattern suggests that multiple small faults or fault segments are rupturing in each swarm rather than a single larger fault. Nonetheless, the waveforms from events within each swarm exhibit similar characteristics (Figure 10).

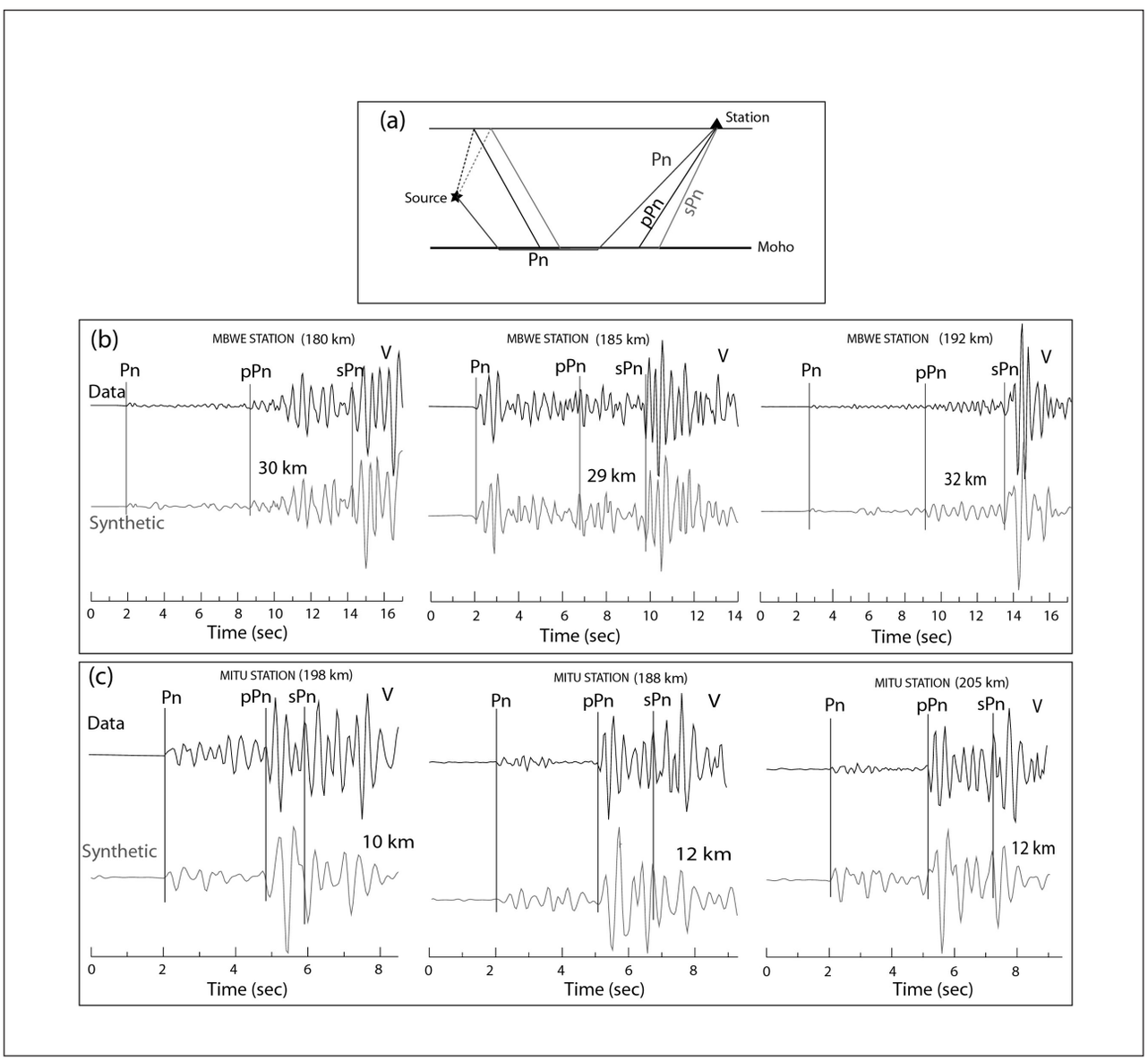


Figure 11. *(**a**) Sketch showing sPn, pPn and Pn travel paths. Selected examples comparing observed vertical displacement seismograms with synthetic seismograms and regional depth phases sPn and pPn for (**b**) three events in the Manyara swarm and (**c**) three events in the KwaMtoro swarm. The numbers above the synthetic seismograms give the focal depths, and numbers next to the station name are epicentral distances.*

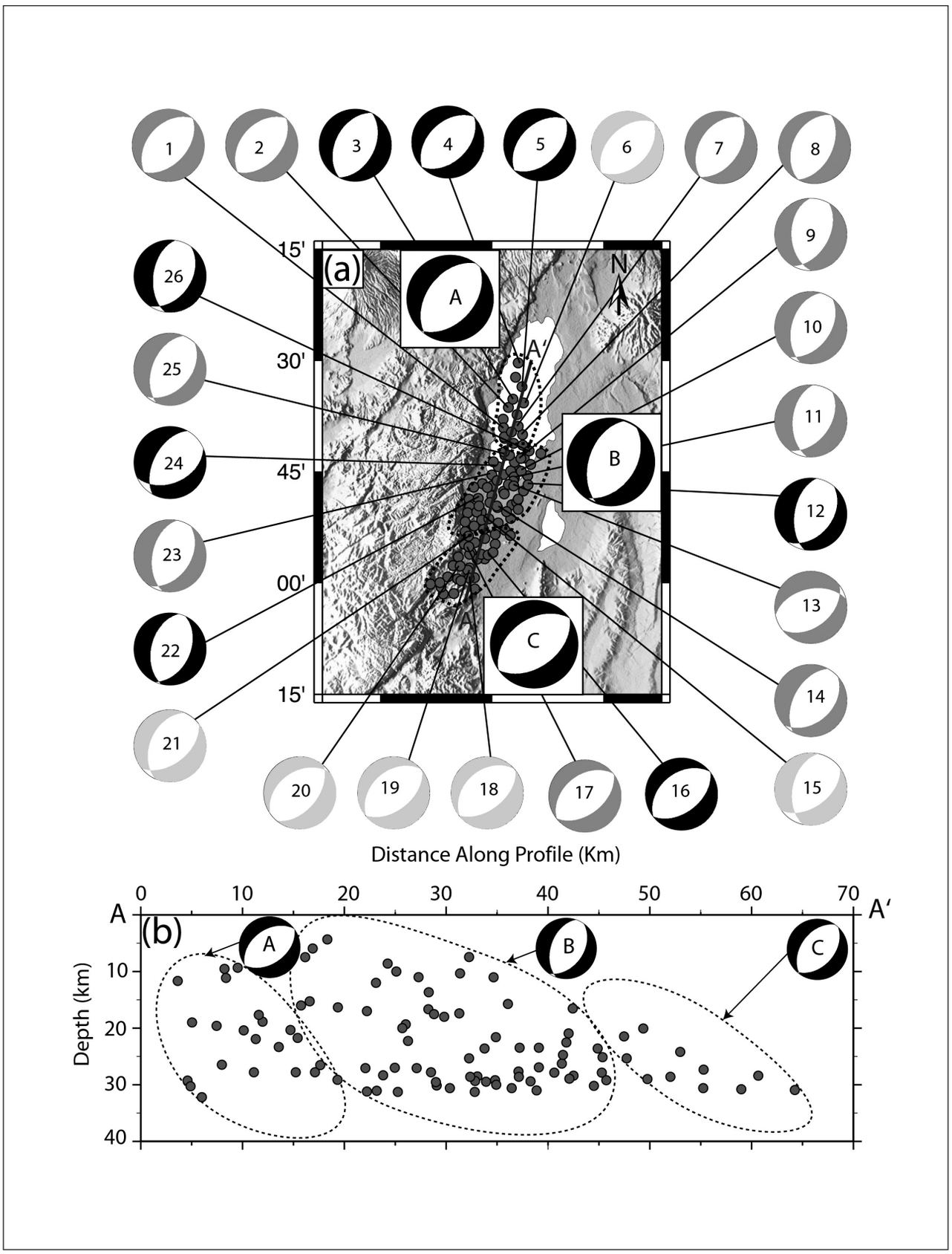


Figure 12. *(**a**) Focal mechanisms from the Manyara swarm. Dotted lines show three identified groups of focal mechanisms whose composite focal mechanisms are shown as A, B and C in the rectangular insets. (**b**) Cross section A-A' of the events drawn parallel to the cluster showing the three groups of the focal mechanisms. Event numbers correspond to those given in Mulibo (2009). Focal mechanisms with depth <20 km are shown in light gray color; 20 to 29 km, dark gray color; 30 to 35 km, black color.*

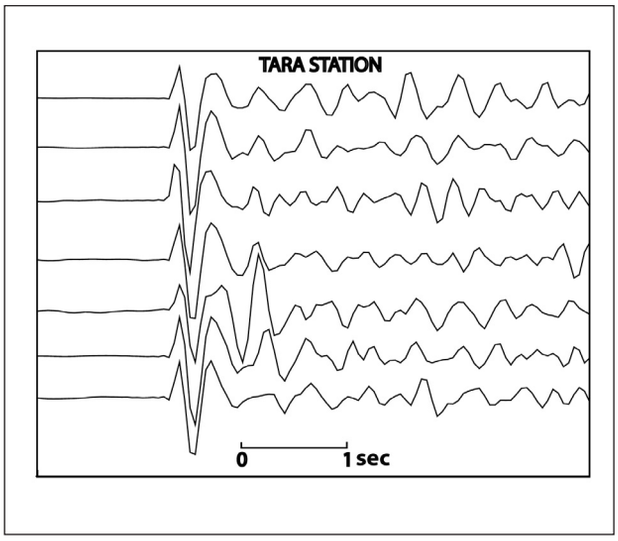


Figure 13. *Selected events with vertical velocity seismograms having similar P wave shapes from focal mechanism of group A in Figure 12.*

Earthquake depths from waveform modeling

Waveform modeling of regional depth phases was done for a number of events to evaluate the accuracy of depths obtained from the location algorithms. Data from three of the deepest events in each swarm were modeled. The best match between the data and synthetic waveform for each event gives a focal depth that is consistent with the one obtained from the location algorithms, indicating that the depth distribution of events is generally well constrained (Figure 11).

Figure 11a illustrates the travel paths of the depth phases modeled, and Figures 11b and 11c show data and synthetics for the events from both swarms. For the Manyara swarm, it can be observed that good matches between the data and synthetic waveforms are obtained at depths of 30 km, 29 km and 32 km, similar to the depths of 31 km, 30 km and 33 km obtained from HYPOELLIPSE. For the KwaMtoro swarm, consistent depths between the waveform modeling and HYPOELLIPSE are also obtained. The synthetic waveforms give depths of 10 km, 12 km and 12 km, consistent with the 11 km, 13 km and 13 km depths obtained from HYPOELLIPSE.

Focal mechanisms

The focal mechanisms for the Manyara swarm show predominantly dip-slip normal faulting (Figure 12). A close examination of the mechanisms shows small variations in the orientation of the nodal planes from north to south along the strike of the swarm. Three groupings of focal mechanisms can be identified for the areas enclosed by the dotted lines in Figure 12 based on similarities in the waveforms and focal mechanisms. Waveforms from events within each grouping have similar P wave shapes, as illustrated in Figure 13. Thus for each of the three groupings, a single focal mechanism was generated by averaging all of the focal mechanisms within each group (Figure 12).

The first two groups (A and B, Figure 12), located in the northern and central parts of the swarm, consist of focal mechanisms striking in a north-northeast to south-southwest direction with a sub eastwest extension direction. Most of the focal mechanisms in group B show a small amount of oblique motion. The third group (C, Figure 12) lies in the southern part of the swarm. The nodal planes in this group strike from the northeast to the southwest. The change in the orientation of the nodal planes between groups A and B and group C is consistent with the change in the orientation of the Manyara rift border fault.

For the KwaMtoro swarm, 24 focal mechanisms have been obtained (Figure 14). The focal mechanisms consistently show northsouth striking nodal planes. A very small amount of oblique motion is shown in some of the mechanisms. The north to south striking nodal planes are consistent with the north to south orientation of the swarm itself and with the major faults and lineaments within the Masai Block (Ring et al., 2005; Figure 3).

Discussion

The events in the Manyara swarm occur at both upper and lower crustal depths and the seismicity pattern and the focal mechanisms correlate well with the orientation of the Manyara border fault. The strong correlation indicates that the events can be associated with slip on the border fault and related faults within the Manyara rift. The Manyara border fault might not extend into the lower crust, but if not, then other faults beneath the rift must extend to depths ≥30 km. Other faults have been shown to be prominent in the vicinity of the Manyara border fault (Ring et al., 2005). The swarm could also be associated with dyke-induced faulting, similar to the 2007 dyke event in northern Tanzania (Baer et al., 2008 and Calais et al., 2009).

Because the KwaMtoro swarm is not associated with any mapped faults, we first investigate if the swarm could be caused by a tensile crack associated with magma intrusion. To do this, three of the events (events 15, 17 and 19) at depths between 9 and 11 km were modeled assuming a crack opening source. The events represent the depths occupied by the majority of the events in the swarm (i.e., 8 to 12 km). First the moment tensor of each event was calculated using the tensile crack opening model and associated cartesian equation from Nakano and Kumagai (2005). Then the polarities of the first P-wave motion for each station were computed using equations (4.83) and (4.91) from Aki and Richards (1980).

The P-wave polarities obtained from the crack model show positive compressional first motions for all stations (Figures 15a to c), which does not match with the observed first motion polarities (Figures 15d to f). From this result, a tensile opening as the source of the seismicity can be ruled out.

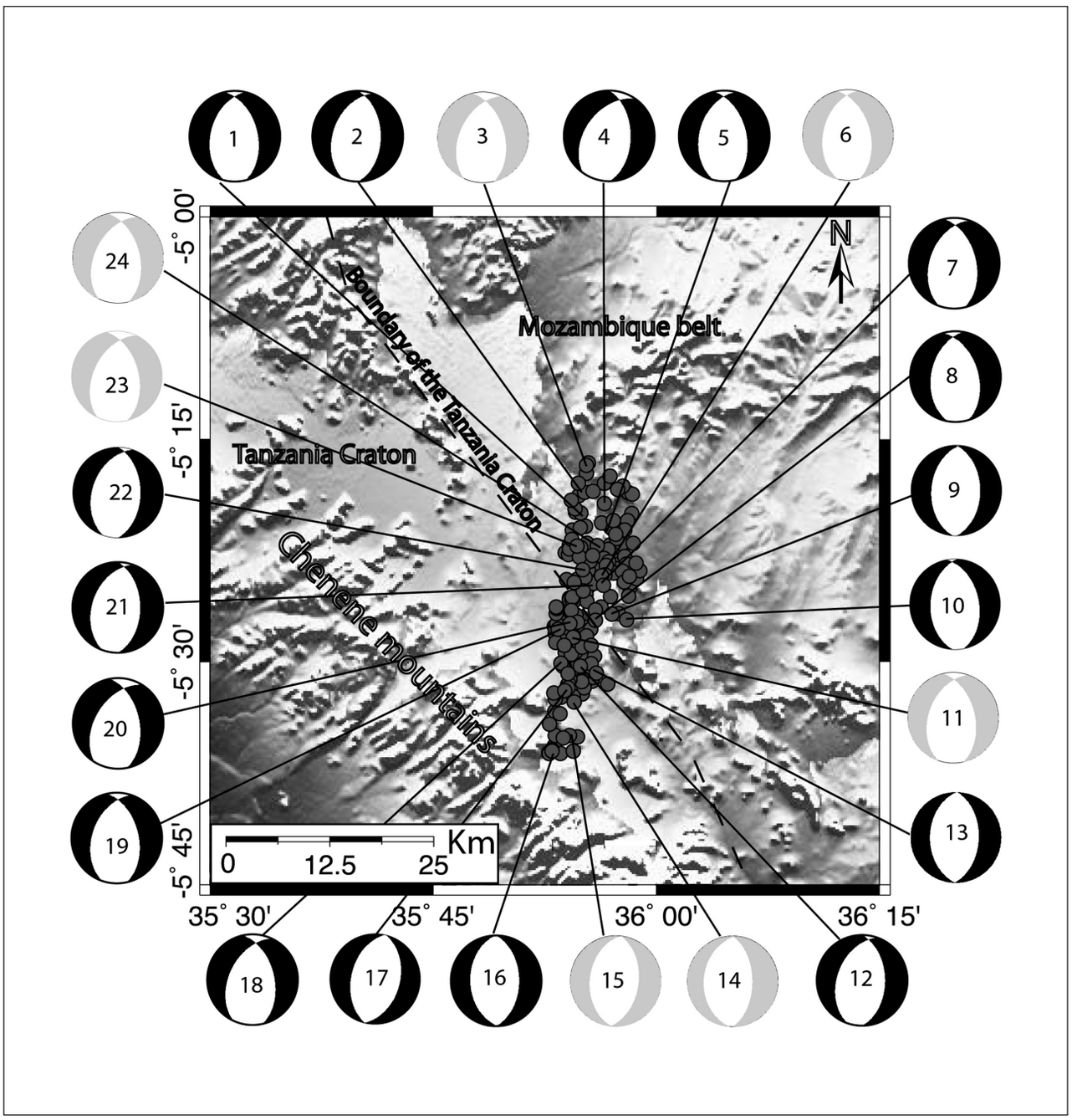


Figure 14. *Map showing focal mechanisms from the KwaMtoro swarm. Events numbers correspond to those given in Mulibo (2009). Focal mechanisms with depth <10 km are shown in light gray color; 10 to 13 km, black color.*

However, a magmatic origin for the swarm might occur in other ways. For example, the swarm could originate from dyke-induced faulting, as in the case of the 2007 dyking event in northern Tanzania (Baer et al., 2008; Calais et al., 2008). Or the presence of magma deep in the crust could cause groundwater movement along shallow fractures resulting in an increase in pore pressure, which would decrease the effective normal stress and thus frictional resistance along a fault (Lengrand et al., 2002). This process can result in an increase in micro-earthquake activity, explained by a decrease of the Coulomb failure envelope around Mohr's circle without changing the orientation of the pre-existing faults (Hubbert and Rubey, 1959).

The alternative possibility is that the KwaMtoro swarm could result from slip along subsurface faults caused by the regional stress field. This possibility is supported by the general north to south orientation of faults in the vicinity of the swarm (Figure 3), similar to the north to south orientation of the swarm itself and the north to south orientation of nodal planes in the focal mechanisms. In Figure 3, many north to south and north-northeast to south-southwest striking faults and lineaments can be seen to the north and east of the

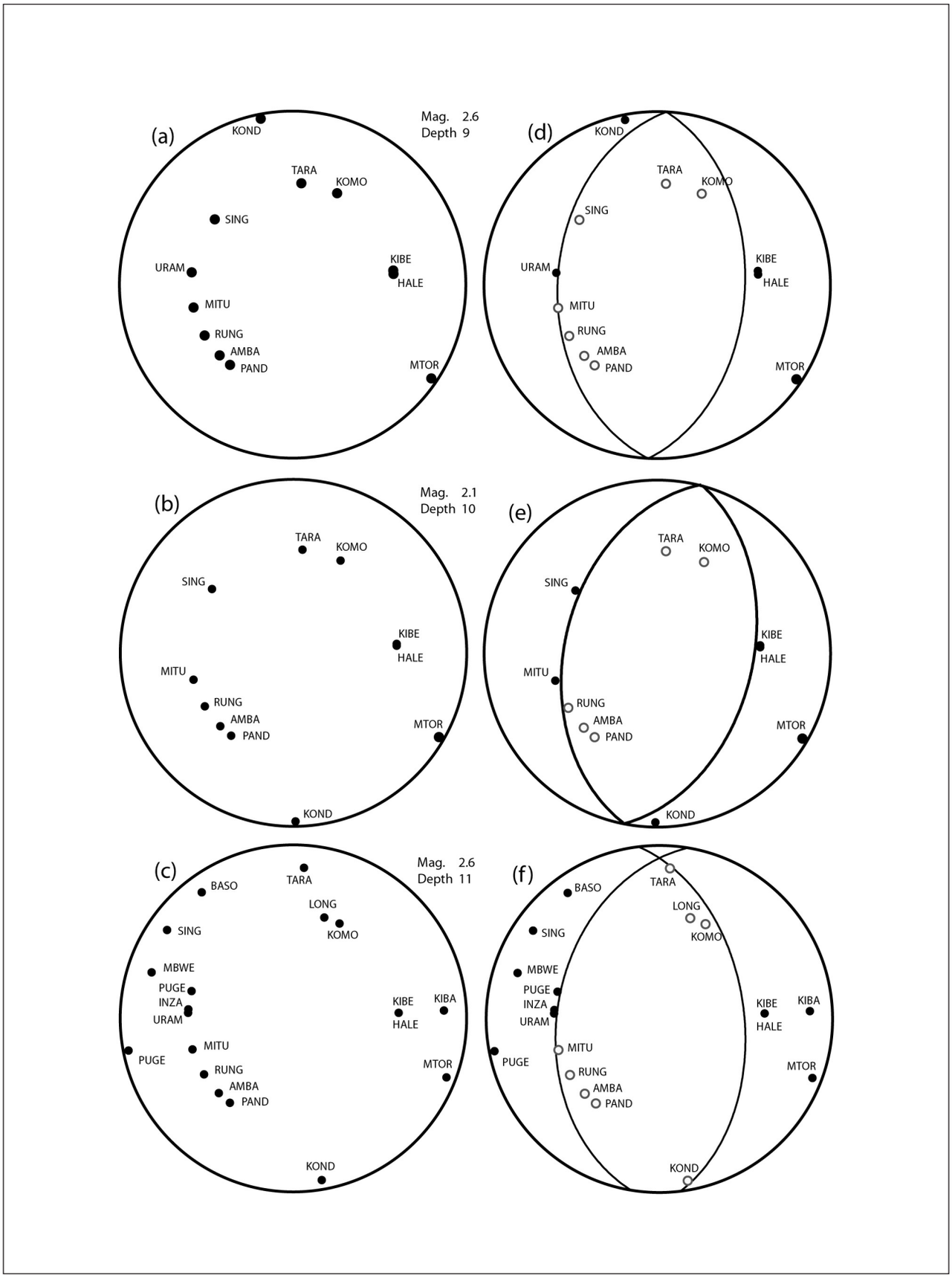


Figure 15. *First motion polarities of P-waves for (**a** to **c**) the solution obtained from the opening crack model and (**d** to **f**) observed polarities and the preferred focal mechanisms for events 15, 17 and 19 in Figure 14. Solid circles show compressional first motions and open circles show dilatational first motions.*

swarm, some not more than a few 10s of kms away from the swarm. Fault lines can also be traced extending from the southern end of the Manyara Rift southward to the KwaMtoro swarm (Figures 2 and 3). Thus, it is likely that a new north to south striking set of rift faults could be developing and giving rise to the earthquake swarm.

As noted in the introduction, the range of source depths reported for East Africa, including northern Tanzania, include many events that have nucleated within both the upper and lower crust (Shudofsky et al., 1987; Nyblade and Langston, 1995; Zhao et al., 1997; Foster and Jackson, 1998; Langston et al., 1998). Strength envelope models show that the thermal structure of the East African lithosphere can support elastic deformation extending to lower crustal depths (Nyblade and Langston, 1995). Thus, the variability in the depth distribution of seismicity between these two swarms is not unexpected.

Summary

From our analyses, we have found that the orientation of the Manyara earthquake swarm correlates well with the Manyara border fault and that focal mechanisms of many events in this swarm are consistent with normal faulting along nodal planes having the same north-northeast orientation as the Manyara border fault. This result indicates that the events are consistent with slip on the border fault and related faults within the Manyara Rift. Either the Manyara border fault or other faults beneath the rift extend to depths ≥30 km. The KwaMtoro swarm cannot be correlated with any mapped faults, and the events are distributed at shallow depths, most of which occur in a depth range of 10 to 12 km. The strong correlation between the north to south orientation of the KwaMtoro swarm, the north to south orientation of nodal planes in many focal mechanisms, and north-south striking extensional structures nearby, indicate that slip along newly developing faults within the subsurface is possible. However, a magma-driven origin for the swarms cannot be ruled out either.

Acknowledgements

We would like to thank the IRIS PASSCAL Instrumental Center and the Tanzania Geological Survey (Ministry of Energy and Minerals) for logistical support in the field during the Tanzania broadband seismic experiment. We would like to thank Cindy Ebinger and an anonymous reviewer for constructive comments. We also thank Sridhar Anandakrishnan and Charles J. Ammon for comments on an earlier version of this paper, and Charles J. Ammon for help with the tensile crack modeling. This research was funded by the National Science Foundation (grants EAR-9304555 and OISE 0530062).

References

Aki, K. and Richards, P.G (1980). Quantitative Seismology, *Freeman and Co., New York*, **37**, 121.

Baer, G., Hamiel, Y., Shamir, G. and Nof, R., (2008). Evolution of a magma-driven earthquake swarm and triggering of the nearby Oldoinyo Lengai eruption, as resolved by InSAR, ground observations and elastic modeling, East African Rift, 2007, *Earth and Planetary Science Letters*, **272**, 339–352.

Brazier, A.R, Nyblade, A.A. and Florentin, J. (2005). Focal mechanisms and the stress regime in northeast and southwest Tanzania, East Africa, *Geophysical Research Letter,* **32**, L14315, doi:10.1029/2005GL023156.

Bungum, H. and Nnko, A.A. (1984). Seismicity and tectonics of the Stiegler's gorge area, Tanzania, *Journal of Geophysical Research,* **89**, 1987–1888.

Burke, K. (1996). The African Plate, *South African Journal of Geology*, **99**, 341–410.

Calais, E., d'Oreye, N., Albaric, J., Deschamps, A., Delvaux, D., Déverchère, J., Ebinger, C.J., Ferdinand, R.W., Kervyn, F., Macheyeki, A., Oyen, A., Perrot, J., Saria, E., Smets, B., Stamps, D.S. and Wauthier, C. (2008). Aseismic strain accommodation by slow slip and dyking in a youthful continental rift, East Africa, *Nature*, **456**, doi:10.1038/nature07478.

Crotwell, H.P., Owens, T.J. and Ritsema, J. (1999). The Taup Toolkit: Flexible seismic travel-time and raypath utilities, *Seismological Research Letters,* **70**, 154–160.

Dawson, J.B. (1992). Neogene tectonics and volcanicity in the north Tanzania sector of the Gregory rift valley: Contrast with the Kenya sector, *Tectonophysics,* **204**, 81.

Ebinger, C.J., Deino, A.L, Tesha, A. L, Becker, T. and Ring, U. (1993). Tectonic controls of rift basin morphology: Evolution of the northern Malawi (Nyasa) rift, *Journal of Geophysical Research,* **98**, B10, 17821–17836.

Ebinger, C.J, Poudjom Djomani, Y., Mbede, E. and Foster, A. (1997). Rifting Archean lithosphere: The Eyasi-Natron-Manyara rift, East Africa, *Journal of Geophysical Society, London,* **154**, 947–960.

Fairhead, J.D. and Girdler, R.W. (1969). How far does the rift system extend through Africa? *Nature*, **221**, 1018–1020.

Fairhead, J.D. and Stuart, G.W. (1982). The seismicity of East African Rift System and comparison with other continental rifts, *Tectonophysics,* **133**, 277–285.

Foster, A.N., Ebinger, C.J., Mbede, E. and Rex, D. (1997). Tectonic development of the northern Tanzania sector of the East African Rift System, *Journal of Geological Society, London,* **134**, 689–700.

Foster, A.N. and Jackson, J.A. (1998). Source parameters of large African earthquakes: implications for crustal rheology and regional kinematics, *Geophysical Journal International,* **134**, 422–448.

Fozzard, P.M.H. (1961). KwaMtoro, Quarter Degree Sheet 123, 1:125,000, *Geological Survey of Tanganyika, Dodoma.*

Hubert, M.K. and Rubey, W.W. (1959). Role of fluid pressure in mechanics of overthrust faulting: I. Mechanics of fluid-filled porous solids and its application to over thrust faulting, *Geological Society of America Bulletin*, **70**, 115–166.

Iranga, M.D. (1992). Seismicity of Tanzania: Distribution in time, space, magnitude and strain release, *Tectonophysics*, **209**, 313–320.

Kebede, F. and Kulhanek, O. (1991). Recent seismicity of the East African Rift System and its implications, *Physics of the Earth and Planetary Interior,* **68**, 259–273.

Kennett, B.L.N. (1983). Seismic Wave Propagation in Stratified Media, *Cambridge University Press, Cambridge, United Kingdom,* 342pp.

Lahr, J. C. (1999). HYPOELLIPSE Y2K: A computer program for determining local earthquake hypocentral parameters, magnitude, and first-motion pattern, U.S. *Geological Survey Open-file Report,* 99–023, 112.

Langston, C. A., Brazier, R., Nyblade, A.A. and Owens, T.J. (1998). Local magnitude scale and seismicity rate for Tanzania, East Africa, *Bulletin of the Seismological Society of America,* **88**, 712–721.

Langston, C. A., Nyblade, A.A. and Owens, T.J. (2002). Regional wave propagation in Tanzania, East Africa, *Journal Geophysical Research*, **107(B1)**, doi:10.1029/2001 JB000167.

Le Gall, B., Nonnotte, P., Rolet, J., Benoit, M., Guillou, H., Mousseau-Nonnotte, M., Albaric, J. and Deverchère, J. (2008). Rift propagation at craton margin. Distribution of faulting and volcanism in the North Tanzania Divergence (East Africa) during Neogene times, *Tectonophysics*, **448**, 1–19.

Lengrand, D., Calahorrano, A., Guillier, B., Rivera, L., Ruiz, M., Villagomez, D. and Yepes, H. (2002). Stress tensor analysis of the 1998-1999 tectonic swarm of northern Quito related to the volcanic swarm of Guagua Pinchincha volcano, Equador, *Tectonophysics*, **344**, 15–36.

Macheyeki, A.S., Delvaux, D., De Batist, M. and Mruma, A. (2008). Fault kinematics and tectonic stress in the seismically active Manyara-Dodoma Rift segment in central Tanzania-Implications for the East African Rift, *Journal of African Earth Sciences*, doi: 10.1016/j.jafrearsci.2008.01.007.

Mulibo, G.D. (2009). The origin of earthquake swarms along the Eastern branch of the East African Rift System in Tanzania, *M.S thesis, Pennsylvania State University, United States of America*, 52pp.

Nakano, M., and Kumagai, H. (2005). Waveform inversion of volcano-seismic signals assuming possible source geometries, *Geophysical Research Letter*, **32**, L12302, doi:10.1029/2005GL022666.

Nyblade A.A. and Brazier R.A. (2002). Precambrian lithospheric controls on the development of the East African rift system. *Geology*, **30**, 755–758.

Nyblade, A.A. and Robinson, S.W. (1994). The African superswell, *Geophysical Research Letter,* **21**, 765–768.

Nyblade, A.A. and Langston, C.A. (1995). East African earthquakes below 20 km depth and their implications for crustal structure, *Geophysical Journal International,* **121**, 49–62.

Nyblade, A.A., Birt, C., Langston, C.A., Owens, T.J. and Last, R.J. (1996). Seismic experiment reveals rifting of craton in Tanzania, *Eos Transactions of the American Geophysical Union,* **77**, 517–521.

Nyblade A.A. and Brazier R.A. (2002) Precambrian lithospheric controls on the development of the East African rift system. *Geology*, **30**, 755–758.

Ring, U., Schwartz, H.L., Bromage, T.G. and Sanaane, C. (2005). Kinematic and sedimentological evolution of the Manyara Rift in northern Tanzania, East Africa, *Geological Magazine*, **142**, 355–368.

Shudofsky, G.N. (1985). Source mechanisms and depths of East Africa earthquakes using Rayleigh-wave inversion and body-wave modeling, *Geophysical Journal of Royal Astronomical Society*, **83**, 563–614.

Shudofsky, G.N., Cloetingh, S., Stein, S. and Wortel, R (1987). Unusually deep earthquakes in East Africa: constraints on the thermo-mechanical structure of a continental rift system, *Geophysical Research Letters*, **14**, 741–744.

Snoke, J.A (2003). FOCMEC: focal mechanism determinations. *In:* W.H.K. Lee, H. Kanamori, P.C. Jennings and C. Kisslinger (Editors), International Handbook of Earthquake and Engineering Seismology, (Chapter 85.12), *Academic Press, San Diego, United States of America*. 1000pp.

Strecker, M.R., Blisniuk, P.M. and Eisbacher, G.H (1990), Rotation of extension direction in the central Kenya rift, *Geology,* **18**, 299–302.

Tesha, A.L., Nyblade, A.A., Keller, G.R. and Doser, D.I (1997), Rift localization in suture-thickened crust: evidence from Bouguer gravity anomalies in northeastern Tanzania, East Africa, *Tectonophysics*, **278**, 315–328.

Waldhauser, F. and Ellsworth, W.L (2000), A double-difference earthquake location algorithm: Method and application to the northern Hayward Fault, California, *Bulletin of the Seismological Society of America*, **90**, 1353–1368.

Wohlenberg, J (1969), Remarks on the seismicity of East Africa between 4N-12S and 23E-40E, *Tectonophysics*, **8**, 567–577.

Zhao, M., Langston, C.A., Nyblade, A.A. and Owens, T.J (1997), Lower-crustal rifting in the Rukwa graben, East Africa, *Geophysical Journal International*, **129**, 412–420.

Editorial handling: R.J. Durrheim